Electronic Supplementary Information

Macromolecular Crowding Effect on the Structure, Function, Conformational Dynamics and Relative Domain Movement of a Multi-Domain Protein as a function of Crowder Shape and Interaction

Nilimesh Das and Pratik Sen*

Department of Chemistry, Indian Institute of Technology Kanpur, Kanpur – 208 016, UP, India
*Corresponding author, E-mail: psen@iitk.ac.in; Fax: +91-512-259-6808

Contents:

Section S1. Synthesis of *p*-nitrophenyl coumarin ester (NPCE)

Equimolar amount of coumarin-343, para-nitrophenol and 4-dimethylamino pyridine (DMAP) was taken in dichloromethane and stirred them in an ice bath for 10 mins. Equimolar N,N-dicyclohexylcarbodiimide (DCC) was added under nitrogen atmosphere while stirring. The solution was stirred at 0°C in an ice bath for further 20 mins and then at 20°C for 24 hours. We then washed the organic layer with ~35 mL 1.2M HCl and then with 35 mL saturated $NaHCO_3$ solution. It was then dried over $MgSO_4$. We then suspended the residue in methanol and washed the precipitate with 100 mL of methanol to remove the unreacted coumarin-343. The precipitate was collected in dichloromethane, dried under vacuum and characterized by ^{1}H-NMR, IR and mass spectrometry.

Section S2. Labelling of HSA with NPCE

We dissolved 50 mg of HSA and 0.4 mg of NPCE in 9 mL of 50 mM phosphate buffer (pH = 8.0) and in a minimum volume of DMSO, respectively. These two solutions were very slowly mixed while stirring. The reaction mixture was then stirred at the room temperature for 30 hrs. Then dialysis was done to remove any untagged dye against 500 mL of 1:15 (v/v) DMSO:buffer (pH 7.4, 50 mM phosphate buffer) solution at 5 °C for 4 days and then against only phosphate buffer for another 4 days. We changed the dialysis medium every 12 hours and recorded the fluorescence of the dialysis medium to check the extent of dialysis.

Section S3. Site selectivity of NPCE tagging

There are altogether 19 tyrosine resideus present in HSA. However, Tyr-411 is the most accessible one at pH 8 for esterification reaction owing to its considerably low pK_a value. The ratio of the protein and the dye (NPCE) is taken as 1:0.87 to avoid tagging of NPCE at multiple sites. The blue shift of NPCE of 7 nm and 9 nm in the absorption and emission spectra respectively proves that it enters more hydrophobic protein matrix as compared to water (Figure S1). We have calculated the ratio of HSA:NPCE in the tagged protein to be 0.85. At reaction condition (pH = 8) Tyr-411 is way more reactive than the other tyrosine residues. Combining these two facts, we can confirm the selective tagging. The fact that the diffusion time of NPCE tagged to HSA (121 μs) is much higher as compared to free NPCE in the buffer (21 μs) also proves the tagging. From FRET experiment, the distance between Trp-

214 and NPCE tagged to Tyr-411 was calculated to be 24 Å, which is very similar to what is obtained from crystal structure and matches well with previous reports.

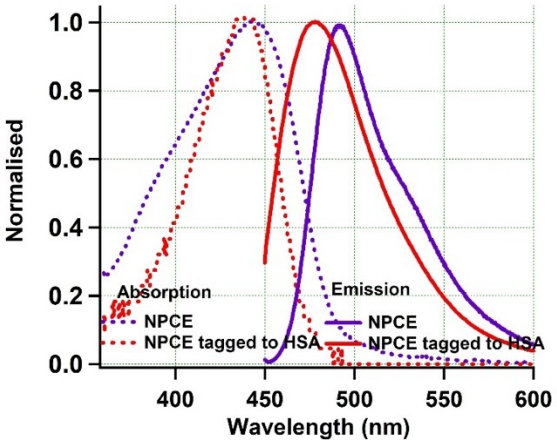

Figure S1. Normalised absorption (dotted line) and emission spectra (solid line) of free NPCE (purple) and NPCE tagged to HSA (red).

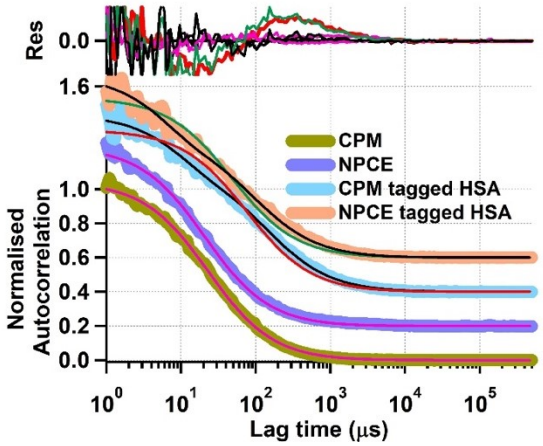

Figure S2. Fluorescence intensity autocorrelation curve of free CPM, free NPCE, CPM tagged to HSA and NPCE tagged to HSA in phosphate buffer. The autocorrelation function of CPM and NPCE is fitted well with equation 1 of the main text. The fitting lines and the residuals are shown in the figure. The autocorrelations of CPM tagged to HSA and NPCE tagged to HSA cannot be fitted with equation 1 satisfactorily, but fitted well with equation 2 (see the fitting lines and residual).

Section S4. Site selectivity of CPM tagging

Human serum albumin contains 35 cysteine residues. Among these only Cys-34 in the domain-I is free and all the others formed a disulphide bond. Thus we expect a site specific tagging of CPM to the Cys-34 residue. For this purpose, we have used HSA and dye in 1:1 ratio so that there does not remain any extra dye in the reaction mixture. The tagging efficiency was calculated to be 0.85 using standard procedure. CPM itself is a very weakly

fluorescent molecule with its emission maximum lies around 481 nm. When tagged to HSA, it shows a blue shift of 16 nm (figure S3). This hints that upon tagging CPM goes inside the protein core. A similar FCS experiment (as that of free NPCE and NPCE tagged HSA) with free CPM and CPM tagged to HSA suggests the tagging (Figure S2). The site-specificity might also be proved from FRET experiment. As discussed in the main text, Trp-CPM forms a very good FRET pair that can give information about the domain-I-domain-II distance of HSA. The distance between CPM attached to Cys-34 of domain-I of HSA and Trp-214 of domain-II of HSA is calculated to be 25 Å. The value matches well with the value from crystal structure.

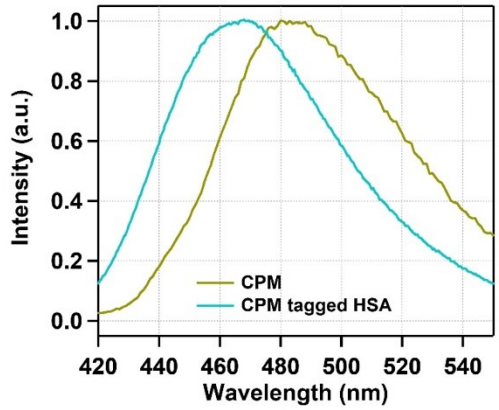

Figure S3. Intensity normalised emission spectra of free CPM and CPM tagged to HSA

Section S5.

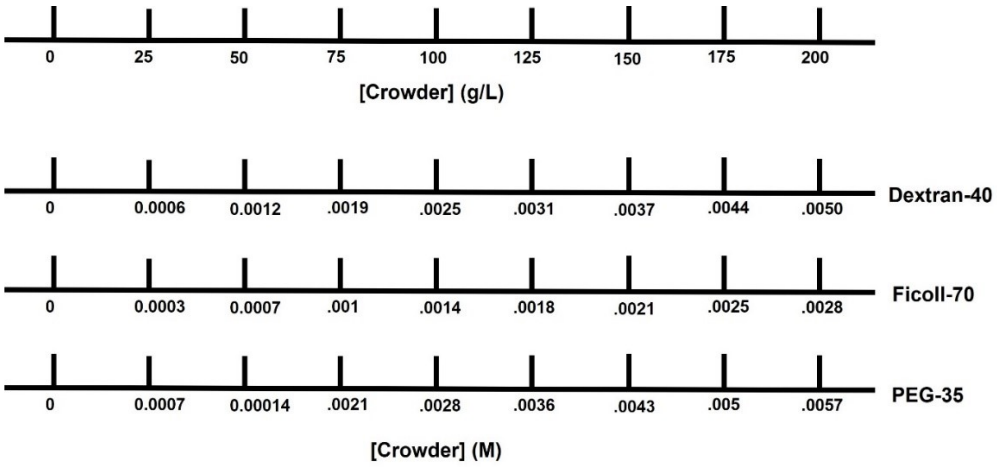

Figure S4. Concentrations of various crowders used in this study. For qualitative comparison purposes, and to keep harmony with previous reports, we have expressed the concentrations in gL^{-1} throughout. However, as molecular weights are different; their molar concentrations will be different.

Section S6. Fluorescence correlation spectroscopic experimental set-up

FCS experiments were done with a home built FCS set-up. An inverted confocal microscope (Olympus IX-71, Japan) with a 60X, 1.2 NA water immersion objective (UplanSApo, Olympus, Japan) along with an excitation source of 405 nm laser source (5 mW, PSU-III-FDA, Optoelectronics Tech. Co. Ltd., China) was used to create a confocal volume. Other components of the system were a multimode fiber patch chord of 25 μm diameter (M67L01 25μm 0.10NA, ThorLabs, USA), dichroic mirror (ZT532rdc, Chroma Tech. Corp., USA), emission filter (605/70m, Chroma Tech. Corp., USA), a photon counting module (SPCM-AQRH-13-FC, Excelitas Tech. Inc., Canada), and a correlator card (Flex99OEM-12/E, Correlator.com, USA). The sample was kept on a cover-slip (Blue Star, Polar Industrial Corporation) on the sample platform. The focal point was set at a distance of 40 μm above the upper surface of the cover slip. The power was optimized to have the best count but no photobleaching. The emitted photons were directed towards the detector through the fibre patch chord. The detected photons were received and autocorrelated by the correlator card and displayed on LabVIEW platform on a computer. Temperature dependent FCS experiments were carried out using specially designed glass cell and the temperature was controlled using Labocon LLCB-202 temperature controller unit.

Section S7. FCS data fitting procedure

Autocorrelation function $G(\tau)$ that arises because of the temporal fluctuation of the fluorescence intensiy can be described as,

$$G(\tau) = \frac{\langle \delta F(t) \delta F(t+\tau) \rangle}{\langle F(t) \rangle^2} \quad \text{(S1)}$$

The autocorrelation is the self-similarity of fluorescence intensity at different times. $\langle F(t) \rangle$ is the average fluorescence intensity, and $\delta F(\tau)$ and $\delta F(t+\tau)$ are the quantity of fluctuation in intensity around the mean value at time t and $(t+\tau)$;

$$\delta F(t+\tau) = F(t+\tau) - \langle F(t) \rangle \quad \text{(S2)}$$

For a single component system, the diffusion time (τ_D) can be obtained by fitting the autocorrelation function $G(\tau)$ using the following equation

$$G(\tau) = \frac{1}{N}\left(1 + \frac{\tau}{\tau_D}\right)^{-1}\left(1 + \frac{\tau}{\omega^2\tau_D}\right)^{-1/2} \quad \text{(S3)}$$

Where, N is the number of particles in the observation volume and $\omega = l/r$ is the longitudinal to transverse radius ratio of the 3D Gaussian volume. If the diffusing species undergoes any other process having amplitude A and timescale τ_R that gives rise to additional fluorescence fluctuation, the modified correlation function can be written as:

$$G(\tau) = \frac{1}{N}\left(1 + \frac{\tau}{\tau_D}\right)^{-1}\left(1 + \frac{\tau}{\omega^2\tau_D}\right)^{-1/2}\left(1 + A \cdot exp\left(-\frac{\tau}{\tau_R}\right)\right) \quad \text{(S4)}$$

We estimated the detection volume to be 0.45 fL using the equation

$$V_{eff} = \pi^{\frac{3}{2}} r^3 \omega \quad \text{(S5)}$$

Section S8. Viscosity and refractive index correction for FCS data

With the addition of crowders, refractive index and viscosity of the solution may change significantly in addition to the diffusion of the solute. We have rectified the effect of the viscosity change by performing a control experiment at every experimental point, taking rhodamine-6G (R6G) as the fluorophore. R6G is a rigid molecule and will not go through any structural change when exposed to the crowder or heat. In this way, any change in its diffusion time through the detection volume will be exclusively because of the change in the medium viscosity. Using this information and the reported value of the hydrodynamic radius of R6G (7.7 Å) in pH 7.4 buffer, we can calculate the hydrodynamic radius of HSA at every experimental point according to the following equation.

$$r_H^{HSA} = r_H^{R6G} \times \frac{\tau_D^{HSA}}{\tau_D^{R6G}} \quad \text{(S6)}$$

The change in the refractive index is compensated by changing the objective collar position and setting it to have the highest G(0) value for each of the samples. In this way, we maintain the lowest detection volume.

Section S9. Secondary structural content of HSA upon NPCE and CPM tagging

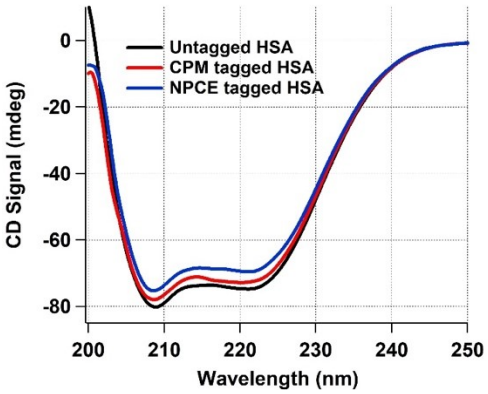

Figure S5. Circular dichroism spectra of untagged, NPCE tagged, and CPM tagged HSA.

Table S1. Secondary structural parameters of untagged HSA, NPCE tagged HSA and CPM tagged HSA

	%-of secondary Structural contents			
	α-helicity	**β-sheet**	**β-turn**	**Random coil**
Untagged HSA	68.0	5.9	12.1	14.0
NPCE tagged HSA	64.5	6.4	12.8	16.2
CPM tagged HSA	66.3	6.2	13.2	15.3

Section S10. Tryptophan emission in presence of PEG-35

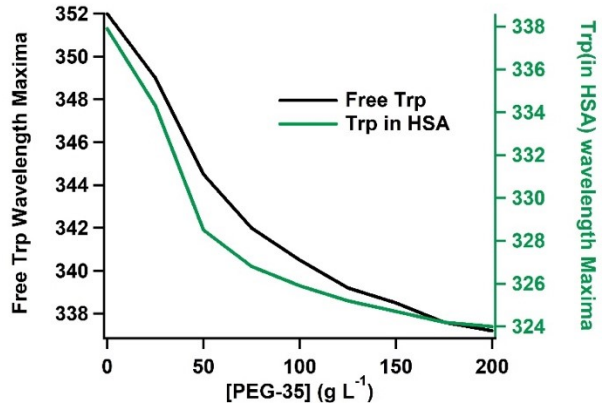

Figure S6. Variation of wavelength maxima of free tryptophan and tryptophan-214 of HSA with increasing concentration of PEG-35.